Transcriptome and metabolome combine to analyze the mechanism of leaf coloration formation in Aeonium arboretum ‘Pink Sybil’

Suhua Li
Suqian University
Rong Zhao
Suqian University
Haozhang Han
21011@squ.edu.cn
Suqian University
Lihua Zhang
Suqian University
Fang Wang
Suqian University
Nan Zhang
Suqian University
Rong Dong
Suqian University

Research Article

Keywords: Aeonium arboretum ‘Pink Sybil’ leaf, coloration, Transcriptome, Metabolome

Posted Date: February 22nd, 2024

DOI: https://doi.org/10.21203/rs.3.rs-3972212/v1

Additional Declarations: No competing interests reported.

Version of Record: A version of this preprint was published at Plant Molecular Biology Reporter on November 28th, 2024. See the published version at https://doi.org/10.1007/s11105-024-01518-6.

Transcriptome and metabolome combine to analyze the mechanism of leaf coloration formation in *Aeonium arboretum* 'Pink Sybil'

Suhua Li[1] · Rong Zhao[1] · Haozhang Han[1,*] · Lihua Zhang[1] · Fang Wang[1] · Nan Zhang[1] · Rong Dong[1]

Abstract

The decorative quality of succulents largely stems from their leaf color. Aeonium arboreum's pink Sybil leaves feature an eye-catching stripe pattern and are particularly favored by customers, although the underlying mechanisms of its distinctive coloration are unknown. This study analyzed *Aeonium arboreum* 'Pink Sybil' leaves at the cellular and molecular levels. UHPLC-HRMS identified 11 flavonoid-related metabolites, showing elevated levels in RS samples. Cyanidin 3-galactoside emerged as the predominant compound, representing 93.4% of the total flavonoid content in RS samples（the red part of leaf margin）, which was substantially greater than in the GM samples（the green part of leaf center）. Freehand slices revealed that anthocyanins, which contribute to the red coloring, were predominantly accumulated in the epidermal cells of the red tissue, in contrast to their presence in the green leaf tissue. Furthermore, cyanidin 3,5-diglucoside was not identified in GM but only in RS. The comparison of two transcripts identified 1,817 DEGs, with 1,123 up-regulated and 694 down-regulated genes. KEGG enrichment analysis revealed that the 20 most significantly enriched DEGs were involved in metabolic pathways, notably the phenylpropanoid and flavonoid biosynthesis pathways, which were closely related to the metabolism of anthocyanins. The majority of the structural genes and transcription factors involved in flavonoid metabolism were shown to be up-regulated using qRT-PCR. Phylogenetic analysis of transcription factors and co-expression network analysis of various metabolites and genes identified one MYB transcription factor, Aa PHL7, and three NAC transcription factors, Aa NAC102, Aa NAC045, and Aa NAC017, which may be involved in the regulation of anthocyanin synthesis in the leaves of the *Aeonium arboreum* 'Pink Sybil'. The expression of these structural genes was highly and positively linked with the levels of anthocyanidins, such as Cyanidin 3,5-diglucoside and Cyanidin 3-galactoside. These compounds synergistically increase the expression of CHS1, CHS2, UFGT1, UFGT2, and 4CL during anthocyanin production. The study's findings identified the primary differential metabolites in the red tissue RS and green tissue GM of *Aeonium arboretum* 'Pink Sybil' leaves. This insight lays the groundwork for the initial identification of structural genes and transcription factors that show a strong and positive link with these metabolites. Our findings pave the way for a deeper understanding of the biochemical processes behind leaf discoloration in *Aeonium arboreum* 'Pink Sybil'.

✉Haozhang Han
21011@squ.edu.cn
[1]School of Information Engineering, Suqian University,
223800 Suqian, Jiangsu, China

Keywords *Aeonium arboretum* 'Pink Sybil' leaf · coloration · Transcriptome · Metabolome

Introduction

The process of color formation is a key area of research in ornamental plants (Wu et al. 2017), as pigmentation influences both the pharmacological activity (Affes et al. 2021) and the visual attractiveness of plants (Yan et al. 2015; Telias et al. 2011). Extensive research indicates that the flavonoid biosynthesis pathway plays a pivotal role in developing plant colors, with anthocyanins acting as the major flavonoid molecules and determining plant color via their species-specific distribution and metabolic processes (Yuan et al. 2023; Liu et al. 2021). Plants have six common anthocyanins, which combine to produce a range of hues from orange-red to violet-blue in flowers. The three principal families of anthocyanins are pelargonidin, cyanidin, and delphinidin, along with their derivatives, peonidin, malvidin, and petunidin, contributing to the pigment diversity and form unique color patterns on organ surfaces (Fang et al. 2015; Davies et al. 2012). Pigmentation is caused by the differential activation of pigment synthesis pathways by epidermal cells in different sections of the tissues. Moreover, anthocyanin distribution patterns may be finely regulated at different developmental stages and regions (Talline et al. 2013). Substantial research has been conducted on the flavonoid biosynthesis pathway that causes anthocyanin accumulation. It has been categorized into three into three distinct steps: anthocyanin biosynthesis, flavonoid biosynthesis, and phenylpropanoid biosynthesis. The process of anthocyanin biosynthesis is facilitated by several enzymes, notably alanine ammonia-lyase (PAL), chalcone synthetase (CHS), chalcone isomerase (CHI), flavanone-3-hydroxylase (F3H), flavonoid-3′-hydroxylase (F3′H), dihydroflavonol-4-reductase (DFR), anthocyanin synthase (ANS), and UDP-flavonoid glucosyltransferase (UFGT). These enzymes are encoded by structural genes (Wang et al. 2023; Li et al. 2023). Transcription factors are as crucial in the production of anthocyanins as structural genes. The MBW ternary complex (Ma et al. 2019) is the most fully investigated regulator of the anthocyanin production pathway. Many structural genes control anthocyanin production, which is directly controlled by the MYB-bHLH-WD40 regulatory factors. Additionally, other transcription factors such as bZIP, WRKY, and NAC also play significant roles in modulating anthocyanin synthesis, either by directly or indirectly affecting the MBW complex (An et al. 2017; Cong et al. 2021; Zhang et al. 2020).

Materials and Methods

Materials

One-year cuttings of the 'Pink Sybil'plant were used in this study. The leaves exhibiting uniform coloration were used particularly those unfolding from the center of the leaf clusters in the fifth and sixth whorls. The green core component (GM) and the red edge part (RS) were separated based on leaf color and immediately froze in liquid nitrogen. Next, the leaves were stored at -80°C before sequencing the transcriptome and metabolome. Each experiment had three biological replicates. Concurrently, the anthocyanin concentration, chlorophyll levels, and leaf structure of both GM and RS sections were measured.

Leaf Anatomy Observations

The slices were created using a rapid freehand slicing technique. Fresh leaves were arranged on a cutting board and precisely sectioned using a pair of parallel double-sided blades, three to four times in succession. The thin slices were then placed in a petri dish filled with distilled water. Each slice was picked up with a brush and deposited in the water droplets on the slides before being covered with a coverslip and the excess water was sucked out using filter paper. A Leica DM500 optical microscope was used to prepare the portions for splicing and imaging.

Determination of Total Anthocyanin and Chlorophyll Content

Following method 2.1, the leaves of GM and RS were meticulously prepared. Each sample, precisely weighed to one gram, was immediately ground into a fine powder using liquid nitrogen. The anthocyanins were extracted into an aqueous solution containing 0.1% hydrochloric acid and allowed to react for four hours at a temperature of 32°C. The absorbance of the filtered extracts was measured at A530 and A657 wavelengths using a spectrophotometer. The anthocyanin content was calculated using the formula: QAnthocyanins=(A530-0.25×A657)×M-1, where M is the fresh weight of the plant material. The entire chlorophyll was extracted using 96% ethanol (v/v). The specific computation was based on the method described by Wellburn and Lichtenthaler (Lichtenthaler et al. 1983).

RNA Extraction and Transcriptome Sequencing

A total RNA kit (Beijing Tiangen Biotechnology Co., Ltd., China) was used to extract total RNA, which was reverse transcribed to cDNA. Following library creation, the fragments were amplified by PCR, the libraries were quality-checked using an Agilent 2100 Bioanalyzer, and the total and effective concentrations were determined using qPCR. Finally, these libraries were sequenced using Next-Generation Sequencing (NGS) technology based on the Illumina sequencing platform for double-end (paired-end, PE).

Transcriptome Data Analysis

CASAVA base recognition was used to transform the image data acquired through a high-throughput sequencer into sequence data (reads) in FASTQ format. Initially, the raw downstream data underwent a filtration process to eliminate reads with junctions, lengths of less than 50 bp, and average sequence quality less than Q20. The high-quality sequences were spliced to generate transcript sequences from scratch. Finally, the transcripts were grouped, and the longest transcript was selected as the unigene. This procedure assured the accuracy and dependability of the data analysis. The Unigene was used for several annotation procedures, including GO, KEGG, eggNOG, SwissProt, Pfam, ORF prediction, and SSR prediction among others. After aligning the filtered sequences to the unigene, the samples were subjected to expression difference analysis, enrichment analysis, cSNP, and InDel analysis to determine the read count number of each unigene.

Metabolite Extraction and Metabolome Analysis

Weigh the sample accurately between 0.1 and 0.5 g, and crush it into a powder using liquid nitrogen. 1 mL of methanol was added to extract around 100 mg of the material. Water: formic acid (70:30:1, v/v/v) was subjected to high-speed centrifugation and sonicated for 20 minutes. The material was

centrifuged at 2000 × g for 10 minutes followed by supernatant filtration through a 0.22 μm nylon filter. The resulting samples were evaluated using Thermo USA's ultra-high-performance liquid chromatography system coupled with its high-resolution Q-extraction mass spectrometry system, the UHPLC-HRMS. The chromatographic column, measuring 50×2.1 mm with a 1.7 μm aqueous HSS T3, was utilized. The mobile phases were 0.1% formic acid-containing ultrapure water and 0.1% formic acid-containing acetonitrile. The flow rate was 0.3 mL/min, the column temperature was 40 °C, the injection volume was 2 μL, and the elution gradient was 0-1 min, 5% B, 1-6 min, 30% B, and 6-8 min, 95% B. The chromatographic separation was performed using electrospray ionization (ESI) with parameters set as follows: the auxiliary gas pressure was 10 arb, the sheath gas pressure was 40 arb, the ion spray voltage was 3000 V, and the temperature was 350°C, which also served as the temperature of the auxiliary gas heater. Both full-scan and positive-ion scanning modalities were utilized. In this study, the gradient dilution technique was employed to create the standard curve for quantitative analysis. The information table for the standard curve is listed in Table S1.

qRT-PCR Identification

Total RNA was extracted from 'Pink Sybil' leaves using the technique described above. The gDNA was extracted, and the cDNA was generated using the EasyScript® One-Step RT-PCR SuperMix (TransGen Biotech, Beijing, China). A LongGene® Q2000B fluorescent quantitative PCR apparatus (LongGene, Hangzhou, China) was used to perform real-time quantitative PCR using a TransStart®Top Green qPCR SuperMix (+Dye II) (TransGen Biotech in Beijing, China). The PCR protocol comprised 39 cycles of 95°C for 30 seconds, 95°C for 5 seconds, and 60°C for 34 seconds yielding a lysis curve. 2-Ct was used to calculate each gene's relative expression. AaACT2 was used as an internal reference gene. The primer sequences involved in this trial are listed in Table S2.

Metabolome-transcriptome Association analysis

Spearman correlation analysis and significance testing of differential metabolites and genes involved in the anthocyanin synthesis pathway in GM and RS samples were performed using GraphPad Prism8. Additionally, Cytoscape 3.7.1 facilitated the creation of network interaction maps for significantly differential metabolites, structural genes, and transcription factors, identified through substantial correlations ($P < 0.05$ and $|r| > 0.7$).

Results and Analysis

Leaf Pigment Distribution and Content Determination

The characteristics of succulent coloration are influenced by the concentration, distribution, and morphology of pigments. Microscopic examination revealed that the leaf blade's core green area (GM) contains a considerable number of water storage cells (Fig. 1C). These cells, containing chloroplasts, exhibit a distinct green coloration. In contrast, the regions on either side of the leaf blade, known as the Red Sides (RS), are almost devoid of chloroplasts, rendering them colorless and transparent. Furthermore, pigmentation was sparingly distributed in the leaf's epidermis in the GM region, particularly in the lower epidermis, and was largely distributed in the cells of 1-2 layers

below the epidermis in the RS region (Fig. 1D). Pigmented cells, enveloped by guard cells, are evident in Figure 1E, alongside visible stomata. The two samples displayed significantly different anthocyanin and chlorophyll levels (Figs. 1G, F), with the GM having 1.84 times more chlorophyll than the RS and the RS having 7.91 times more anthocyanin than the GM. The RS tissue has a much greater anthocyanin content than the GM tissue.

Metabolomics Analysis of Flavonoids

The UHPLC-HRMS study of anthocyanin-related metabolites revealed the presence of 12 anthocyanin glycosides in GM and RS samples. These comprised six anthocyanins: Cyanidin 3-galactoside, Cyanidin 3,5-diglucoside, Cyanidin, Petunidin, Malvidin, and Peonidin (Fig. 2A); three flavonols: Rutin, Quercetin, and Kaempferol (Fig. 2B); two flavonoids: Luteolin and Isorhamnetin (Fig. 2C); and Procyanidin B2 (Fig. 2D). Except for rutin, the metabolite levels of the RS samples were considerably greater than those of the GM, as determined by the statistical significance of the difference observed. Cyanidin 3-galactoside was the most abundant, with a concentration of 12,487 ng/g in RS samples, representing 93.4% of the total flavonoid content. Furthermore, cyanidin 3,5-diglucoside was only discovered in the red tissue (RS) and not the green leaf tissue (GM). This research implies that Cyanidin 3,5-diglucoside and Cyanidin 3-galactoside play a distinct function in the anthocyanin accumulation of 'Pink Sybil'leaves and that these pigments are principally responsible for the leaves' red color.

Transcriptome analysis

Transcriptome Sequencing and Assembling

The RS and GM libraries yielded 45,731,216 and 4,424,978,5clean reads, respectively, after removing linkers and low-quality reads (Clean Data%≤90.93, Table S3). Trinity software was used to generate a total of 267585 transcripts with an average length of 104 0bp and a N50 of 1403 bp, as well as 84,750 single genes with an average length of 857 bp and a N50 of 1151 (Table S4). The transcriptome PCA findings are shown in Figure S1. Six samples were divided into two groups, with significant relationships observed among the duplicates within each group. The significant difference between the groups shows that the metabolome data is credible. Functions of all single genes were annotated with several reference databases. The NR, GO, KEGG, Pfam, eggNOG, and SwissProt databases were annotated for 54,040, 38,971, 25,062, 24,425, 55,348, and 42,038 Unigenes. In the eggNOG and NR databases, more unigenes (65.31% and 63.76%, respectively) were effectively annotated. A total of 9,920 unigenes, constituting 11.71%, were successfully matched across all six databases. The annotation of gene sequences from *Aeonium arboreum* 'Pink Sybil' samples against the NR database revealed significant matches with seven species, including 4.35% similar to *Vitis vinifera*, 3.31% to *Nyssa sinensis*, 2.33% to Vitis riparia, 2.30% to *Camellia sinensis*, 1.76% to *Pistacia vera*, and 1.53% to *Tetracentron sinense* and *Hevea brasiliensis*. However, 82.88% of the unigenes could not be matched to the NR database (Figure S2).

Differential Expression Gene Analysis

Differential gene expression was assessed with the screening threshold set at |log2FoldChange| > 1 and P-value < 0.05. The study examined 1,817 DEGs, utilizing Tnm (GM) as the control, identifying 1,123 up-regulated genes and 694 down-regulated genes (Fig. 3A). Subsequent analysis employed topGO for GO enrichment, elucidating the principal biological activities of the DEGs. The top 20 GO word entries with the lowest FDR value, or those with the highest enrichment were chosen for presentation, and genes linked with biological regulation and stimulus-response were highly categorized in the biological process categorization (BPs). Genes involved in biological regulation and stimulus-response were found to be overrepresented among the biological process (BP) categories (Figure S3). The KEGG enrichment analysis identified the top 20 enriched metabolic pathways, providing an enhanced understanding of DEGs' metabolic activities. These activities included the related anthocyanin biosynthesis pathways, flavonoid biosynthesis, and phenylpropanoid biosynthesis (Figure. 3B).

Differential Structural Gene Screening

The DGE analysis examined two samples to identify the structural genes responsible for anthocyanin synthesis in 'Pink Sybil'. Based on KEGG pathway annotations concerning anthocyanin production and DEG expression, we selected fifteen differential genes for transcriptional profiling (Fig. 4). Despite the up-regulation trend, the expression of CHI (TRINITY_DN7885_c0_g1) in RS, FLS (TRINITY_DN57197_c0_g1), and ANR (TRINITY_DN5187_c0_g1) in GM samples remained consistent. Compared to GM, the expression levels of other genes involved in the anthocyanin biosynthesis pathway were significantly higher. Notably, ANS (TRINITY_DN6997_c0_g1), CHS1 (TRINITY_DN5698_c0_g1), UFGT1 (TRINITY_DN4478_c1_g1_i1), UFGT2 (TRINITY_DN6874_c0_g1), F3'H1 (TRINITY_DN984_c0_g1), and F3H (TRINITY_DN29385_c0_g1) demonstrated significant increases in expression. These genes are likely pivotal in conferring the red pigmentation observed in the leaves of 'Pink Sybil'.

Analysis of transcription factors involved in anthocyanin biosynthesisThis study examined five MYBs, one BHLH, and three NAC transcription factors from DEGs in addition to structural genes (Supplementary Table S5). Phylogenetic analysis was conducted on leaves of Aeonium arboreum 'Pink Sybil' to pinpoint potential transcription factors for MYBs and NACs involved in anthocyanin synthesis. The findings revealed that AaMYBs were grouped into four classes, including 11 MYBs from different species (Fig. 5). The study identified four anthocyanin-regulated R2R3-MYB TFs (LfMYB113, VvMYBA2, PpMYB10, and MdMYB10), along with AaMYB114 and AaMYB90, in subgroup 6. Additionally, AaMYB111 and four flavonol-regulated R2R3-MYB TFs (PsMYB12L, VvMYBF1, AtMYB111, and CsMYBF1) were classified under subgroup 7 (Dubos et al. 2010). AaPHL7 and AaMYB-LIKE X are type 1R MYBs and are classified as the third and fourth branches, respectively. Their functions primarily entail the synthesis of flavonoids and anthocyanins (Jiang et al. 2019; Zhang et al. 2023; Lu et al. 2023).

Members of the NAC (NAM, ATAF, and CUC) transcription factor family interact with other transcription factors, hormones, and environmental stimuli and play an important role in anthocyanin production (Wen et al. 2022). The NAC protein family, analyzed across rice (monocotyledonous) and Arabidopsis thaliana (dicotyledonous) by Hisako et al., was classified into 18 subgroups according to sequence similarities. The sequences of ATAF and NAP substructural domain E are highly conserved, indicating potential comparable functions in regulating anthocyanin production, a process associated with stress response (Ooka. 2003). To investigate the relationship between AaNACs and other NACs, a phylogenetic tree was constructed, aligning the genes with those from Oryza sativa and Arabidopsis thaliana following the technique proposed by Hisako et al. (Figure S4). The findings revealed that genes located on the first-formed branch of the developmental tree fall within the ATAF and NAP subgroups, both influential in anthocyanin synthesis (Fig. 6). Subsequently, on the second branch, AaNAC017 was identified to share similarities with LrNAC078 and ANAC078 of the NAC2 subgroup, which favorably controls flavonoid synthesis in high-light conditions (Li et al. 2020; Morishita et al. 2014). The third meristem contains genes that regulate anthocyanin production and PA metabolism. MdNAC14-like belongs to the ANAC001 subgroup, whereas AaNAC045 and MdNAC52 were associated with the ONAC003 subgroup. These genes' transcript levels increase in response to light (Sun et al. 2019). AaTT8 (DN3147_c0_g1) was the sole BHLH-type transcription factor that showed substantial up-regulation. By TAIR comparison, it had the greatest similarity with Arabidopsis AtTT8, and this gene may work with transcription factors such as MYBS to co-regulate anthocyanin production in *Aeonium arboreum* ‘Pink Sybil’ (Xu et al. 2013).

qRT-PCRidentification of DEGs Involved in Anthocyanin BiosynthesisTo evaluate the validity of the RNA sequencing results, quantitative RT-PCR was utilized to analyze 14 essential structural genes and 10 transcription factors involved in the production of anthocyanins in *Aeonium arboreum* ‘Pink Sybil’. Except for AaMYB111 and AaMYB114, all studied genes had significantly different expressions in GM and RS, using AaACT2 as the reference gene. The transcriptional data and the RT-PCR results were mainly in agreement. (Fig. 7).

Metabolome-transcriptome Association analysis

To discover the major factors influencing the synthesis of leaf-colored anthocyanins, the Cytoscape was employed to analyze network interactions among metabolites, key structural genes, and transcription factors within the flavonoid metabolism of *Aeonium arboreum* ‘Pink Sybil’. We screened 12 differential metabolites, 11 structural genes for anthocyanin synthesis, and 4 transcription factors using a threshold (correlation coefficient r) greater than 0.7 to illustrate their associations(Fig. 8A). Significantly, Cyanidin 3,5-diglucoside and Cyanidin 3-galactoside emerged as the most critical metabolites, exhibiting a strong positive correlation (correlation coefficient >0.8) with the majority of the structural genes. The flavonol metabolites (Kaempferol, Isorhamnetin, Quercetin, and Luteolin), as well as the anthocyanins Malvidin and Peonidin, exhibited correlation coefficients lower than 0.8 with all structural genes, indicating that they are not the primary

metabolites for anthocyanin synthesis in ‘Pink Sybil’. Out of the 11 structural genes, 4CL, CHS1, CHS2, UFGT1, and UFGT2 had the greatest influence on the content of anthocyanin metabolites, and exhibited a highly positive correlation (correlation coefficients >0.8) with Cyanidin 3,5-diglucoside and Cyanidin 3-galactoside content, as well as strong correlations between CHS2, and Cyanidin, Procyanidin B2, between 4CL, UFGT2, and petunidin levels (Figure 8C). The analytical findings showed that AtNAC102 and AtNAC045 were positively associated with the expression of most structural genes, having a closer relationship with CHS1, CHS2, UFGT1, UFGT2, and 4CL. Moreover, a significant transcriptional level of AtNAC017 and AaPHL7 was observed, with certain positive connections noted, such as AtNAC017 with PAL and AaPHL7 with CHS2. We generated a network diagram to determine the relationship between structural genes and transcription factors(Figure 8B).

AtNAC102 and AtNAC045 appear to synergize in regulating anthocyanin synthesis in ‘Pink Sybil’ leaves, affecting the expression of key structural genes, such as Cyanidin 3,5-diglucoside and Cyanidin 3-galactoside through the modulation of CHS1, CHS2, UFGT1, UFGT2, and 4CL pathways. Notably, the compounds Cyanidin 3-galactoside and Cyanidin 3,5-diglucoside are central to this regulatory mechanism.

Conclusion and Discussion

Anthocyanins are regarded as the fundamental pigments in plant organs, and leaf color is mostly determined by the differential expression of genes that control pigment production in leaf tissues over both temporal and geographical dimensions. Investigation of various *Ananas comosus* variants revealed that the bracteatus leaf samples displaying a red coloration contained significantly higher anthocyanin levels compared to their green counterparts. RNA-Seq analysis revealed that eleven anthocyanin-related genes were differentially expressed between the two samples (Zhou et al. 2021). Zou et al. reported fourteen DEGs that were positively correlated with anthocyanin accumulation, emphasizing the critical role of anthocyanin in the color transition observed in the inner leaves of ornamental kale (Zou et al. 2023). Our findings suggest that anthocyanins are the major pigments responsible for the red hue of ‘Pink Sybil’ leaves.

The flavonoid and anthocyanin pathways were active in RS (Fig. 3). Analysis of DEGs and differentially accumulated metabolites (DAMs) in the flavonoid pathway, combined with RT-PCR results, revealed significant overexpression of 14 structural genes, including PAL and 4CL, and 11 metabolites, such as Cyanidin 3,5-diglucoside and Cyanidin 3-galactoside. The network interactions analysis graph revealed that three gene types, 4CL, CHS, and UFGT, exhibit higher expression activities in the flavonoid biosynthesis pathway, with a strong positive correlation between their transcript levels and metabolite content. The 14 structural genes, including PAL, 4CL, CHS, UFGT, DFR, and ANS, showed considerable upregulation. According to the flavonoid synthesis pathway, the enzymes PAL, 4CL, and CHS are critical for the biosynthesis of phenylpropanoid, flavonoids, and anthocyanins, respectively. As upstream anthocyanin synthesis genes, 4CL and CHS were required to convert phenylpropanoid into anthocyanin, ensuring an adequate supply of anthocyanin

precursors (Coumaroyl coenzyme A and chalcone), which significantly boosts anthocyanin levels in sweet cherry fruit (Wei et al. 2015). Similarly, colored Tibetan barley showed significantly higher levels of 4CL and CHS expression than colorless types (Yao et al. 2022). The structural genes encode the enzyme UFGT, which completes the anthocyanin production pathway. It converts unstable anthocyanins into stable anthocyanins via glycosylation. In Paeonia, variations in Ph UGT78A22 expression resulted in distinct glycosylation of pigments in the spotted and unspotted regions of the petals, resulting in floral color variations (Li et al. 2022). Furthermore, high expression of UFGT increased the red pigmentation of the fruit skin. This is because UFGT is essential for fruit coloration, including apples (Xue et al. 2021), peaches (Wen et al. 2014), grapes (Koyama et al. 2018), Japanese apricots (Ni et al. 2018) [39], and litchi (Zhao et al. 2012), among others.

When it comes to anthocyanin accumulation, CHI is debatable. A previous study reported that an increase in anthocyanidin content was associated with an increase in CHI activity (Morita et al. 2014; Ryan et al. 2002). Another study found that an increase in CHI activity was not required for an increase in anthocyanidin accumulation. For instance, Zhou et al. discovered that an increase in CHI expression was not required for flavonoid accumulation in *Camellia nitidissima* (Xing et al. 2017). Moreover, it was discovered that transcription factors associated with anthocyanin production control the expression of downstream genes by controlling CHS rather than directly controlling the expression of CHI in peonies (Hong et al. 2022). The current study's findings support the latter theory, with comparable levels of CHI transcripts in the GM and RS samples and no discernible relationship to anthocyanin production in ‘Pink Sybil’ leaves.

In addition to key structural genes, transcription factors such as MYB, bHLH, WD40, and NAC are important in flavonoid biosynthesis. R2R3-MYB proteins, the largest class of MYB transcription factors, play important roles in anthocyanin synthesis in a variety of plants. In Arabidopsis thaliana, AtMYB75, AtMYB90, AtMYB113, and AtMYB114 promote anthocyanin biosynthesis in nutrient tissues (Gonzalez et al. 2010), whereas S7 subgroups AtMYB11, AtMYB12, and AtMYB111 primarily control flavonol biosynthesis in tissues (Stracke et al. 2010). In apples, MdMYB10 controls the fruit and leaf anthocyanin synthesis pathways (Espley et al. 2009) In maple, the R2R3-MYB gene LfMYB113 is responsible for fall leaf coloration (Wen et al. 2017). Similarly, small MYB proteins with single or partial MYB repeat sequences can play a role in anthocyanin biosynthesis. LcR1MYB1 interacts with LcNAC13 to co-regulate lychee anthocyanin biosynthesis-related genes (Jiang et al. 2019), while the transcriptional regulation of flavonoids by VvPHL7 (Zhang et al. 2023) and CnPHL7 (Lu et al. 2023) is mediated by stress signaling, leading to increased transcript levels under conditions of disease or low temperature, respectively. To investigate the transcriptional expression of AaMYBS in ‘Pink Sybil’ leaves, we constructed a phylogenetic tree of MYBs from *Aeonium arboreum* ‘Pink Sybil’ and other species. Preliminary results from homology analysis suggest that AaMYB90, AaMYB114, and AaMYB-LIKE X may play a role in structural anthocyanin synthesis in the leaves of ‘Pink Sybil’genes, AaMYB111 may be involved

in flavonoid biosynthesis, and AaPHL7 in stress responses. However, the combined network interactions analysis revealed that MYBs other than AaPHL7 had low correlation coefficients with flavonoid metabolites, and the R2R3-MYB types AaMYB114 and AaMYB111 were not significantly up-regulated for expression in the RT-PCR assay. The findings of the preceding analyses indicate that transcriptional differences in structural genes between RS and GM samples of ‘Pink Sybil’ leaves may not be directly attributable to R2R3-MYB transcription factors.

Our findings suggest that NAC TF is important for anthocyanin synthesis. The NAC TF, a member of the expansive plant-specific transcription factor families, is increasingly recognized for its regulation of flavonoid production. Specifically, the interaction of LcNAC002 enhances the expression of both LcSGR and LcMYB1 in lychee, facilitating anthocyanin accumulation (Zou et al. 2023). Furthermore, the activation of PpMYB10.1 by the BLOOD (BL) gene, encoding an NAC TF, is essential for anthocyanin synthesis in Prunus persica (Zhou et al. 2015). VviNAC60 and VviMYBA1 interacted in grapes to cause a notable anthocyanin accumulation in immature leaves(D'Incà et al. 2023). High expression of ANAC078 in Arabidopsis caused anthocyanins to accumulate in response to HL stress (Morishita et al. 2014). MdNAC52 and MdNAC14-Like TF in apples bind to the promoters of genes encoding anthocyanin-related MYBs to regulate anthocyanin biosynthesis and bind to the promoter of MdLAR, a structural gene in the PA pathway to regulate PA synthesis (Sun et al. 2019; Xu et al. 2023). We identified four significantly up-regulated NAC TFs using transcriptome analysis and RT-PCR. AaNAC102, a homolog of LcNAC002, may result in a significant up-regulation of structural genes for anthocyanin synthesis in ‘Pink Sybil’ leaves. Notably, AaNAC017, homologous to ANAC078, may be involved in the biosynthesis of flavonoids in ‘Pink Sybil’ leaves; and AaNAC045, homologous to MdNAC52 and MdNAC14-Like with high homology, may contribute to anthocyanin accumulation and PA synthesis. The precise regulatory mechanisms governing key genes involved in phycocyanin synthesis remain to be fully elucidated due to the intricate and complex nature of the regulatory network. Despite notable differences between the two transcript samples, AaNAC073 exhibits limited homology with known transcription factors, as per Tair's analysis, showing the greatest similarity to AtNAC073. The function of AtNAC073, a member of the secondary wall-associated NAC structural protein (Zhong et al. 2008), in the biosynthesis of anthocyanins in ‘Pink Sybil’ leaves has to be further investigated. AaNAC102 and AaNAC045 were more strongly associated with metabolites in the network interaction diagram between transcription factors and structural genes than AaNAC017. This helps to explain why anthocyanins were the main differential metabolites in the ‘Pink Sybil’ GM and RS samples, while other flavonoids were less common.

Network interaction analysis identified four key transcription factors: three NAC transcription factors (AaNAC045, AaNAC102, and AaPHL7), one MYB transcription factor (AaPHL7), that can synergistically promote the upregulated expression of CHS1, CHS2, UFGT1, UFGT2, and 4CL, crucial for anthocyanin synthesis. These structural genes are crucial for the accumulation of anthocyanin anabolic metabolites (Cyanidin 3,5-diglucoside and Cyanidin 3-galactoside).

Phylogenetic analysis suggests that all four transcription factors, AaPHL7, AaNAC102, AaNAC045, and AaNAC017, may participate in the plant's stress response mechanisms. The production of anthocyanin and PA is influenced by abiotic factors, including nutrient availability, phytohormones, and environmental stimuli (Yan et al. 2021). In the case of spotted bougainvillea, the colored parts of the leaves are more susceptible to changes in the environment and stimuli, and adversity stress causes the expression of several genes related to this stress response to be up-regulated (Zhou et al. 2021). Meanwhile, the accumulation of flavonoids helps shield the plant from biotic and abiotic stresses.

The present study focuses on the genes and metabolic pathways associated with anthocyanin synthesis, using transcriptome data and considering both phenotypic and physiological indicators. Nevertheless, the complex composition of leaf color includes carotenoids and chlorophyll in addition to anthocyanin, with the final leaf color resulting from the cumulative effect of these pigments (Tian et al. 2021). The leaf color of 'Pink Sybil' is primarily composed of red and green hues prompting us to quantitatively assess the chlorophyll and anthocyanin content in these areas. Our findings highlight a significant difference in the ratio of anthocyanin to chlorophyll, as the anthocyanin content was significantly higher in the RS sample while the GM sample had significantly lower levels of the two pigments. Consequently, gaining a deeper understanding of the molecular mechanisms behind the leaf coloration in 'Pink Sybil' requires an in-depth investigation of the biosynthetic pathways of these pigments.

In this study, we performed UHPLC-HRMS analysis and transcriptome sequencing of the red central region and red marginal region of the *Aeonium arboreum* 'Pink Sybil' leaves. The findings revealed that the red coloration of 'Pink Sybil' leaves was mainly attributed to the accumulation of Cyanidin 3-galactoside and Cyanidin 3,5-diglucoside. We successfully assembled and annotated 84,750 single genes. Comparative analysis of the transcriptomes identified 1,817 differentially expressed genes, including 1,123 up-regulated genes and 694 down-regulated genes. KEGG enrichment analysis highlighted the most significantly enriched metabolic pathways among 20 DEGs, including flavonoid and phenylpropanoid synthesis pathways closely related to flavonoid metabolism. qRT-PCR analysis verified 14 structural genes related to anthocyanin metabolism and 10 transcription factors, which were consistent with the transcriptome sequencing results. Through comprehensive phylogenetic analysis and co-expression network analysis, we preliminarily identified one MYB transcription factor, AaPHL7, and three NAC transcription factors, AaNAC102, AaNAC045, and AaNAC017, as potential contributors to anthocyanin synthesis in 'Pink Sybil'. Notably, AaNAC102 and AaNAC045 were pinpointed as key genes that may drive the up-regulation of CHS1, CHS2, UFGT1, UFGT2, and 4cl in the anthocyanin synthesis pathway. AaPHL7 and AtNAC017 contribute to flavonoid synthesis, however, their roles in anthocyanin accumulation appear auxiliary. These findings offer valuable insights into the genetic mechanisms underpinning color formation in 'Pink Sybil' leaves, laying a foundation for further research in this area.

Author Contribution LSH and HHZ conceived the idea. ZR and ZLH performed the experiments. LSH, ZR, and HHZ analyzed the data; LSH wrote the manuscript. WF, ZN, and DR constructed and improved the figures. All the authors have read and approved the final version of the manuscript.

Funding This project is jointly funded by the basic science research (natural science) of colleges and universities in Jiangsu province (23KJD210005), Suqian Science and Technology Program (K202207) and the Suqian University Innovation Team Project (2021td05).

Availability of Data and Materials All data generated or analyzed during this study are included in this published article (and its supplementary information files).

References

Wu X, Gong Q, Ni X, et al (2017) The key enzyme associated with the petals variegation in Japanese apricot. Front. Plant Sci.https://doi. org/10.3389/fpls.2017.00108

Affes S, Younes AB, Frikha D, et al (2021) ESI-MS/MS Analysis of Phenolic Compound from Aeonium arboreum Leaf Extracts and Evaluation of their Antioxidant and Antimicrobial Activities.Molecules.https://doi.org/10.3390/MOLECULES26144338

Yan Zhao Z, Yanwei C, Huiyuan Y, et al (2015) Transcriptome sequencing of purple petal spot region in tree peony reveals differentially expressed anthocyanin structural genes. Frontiers in Plant Science.https://doi.org/10.3389/fpls.2015.00964

Telias A, Lin-Wang K, Stevenson DE, et al (2011) Apple skin patterning is associated with differential expression of MYB10. Bmc Plant Biology.https://doi.org/10.1186/1471-2229-11-93

Yuan Y, Li X, Yao X, et al (2023) Mechanisms underlying the formation of complex color patterns on Nigella orientalis (Ranunculaceae) petals. New Phytol. https://doi.org/10.1111/nph.18681

Liu Y, Feng X, Zhang Y, et al (2021) Simultaneous changes in anthocyanin, chlorophyll, and carotenoid contents produce green variegation in pink–leaved ornamental kale. BMC Genomics.https://doi.org/10.1186/s12864-021-07785-x

Fang J (2015) Classification of fruits based on anthocyanin types and relevance to their health effects.Nutrition.https://doi.org/10.1016/j.nut.2015.04.015

Davies KM, Albert NW, Schwinn KE (2012) From landing lights to mimicry: the molecular regulation of flower colouration and mechanisms for pigmentation patterning. Functional Plant Biology.https://doi.org/10.1071/FP12195

Talline RM, Jeremy JB, Steven B, et al (2013) Precise spatio-temporal regulation of the anthocyanin biosynthetic pathway leads to petal spot formation in Clarkia gracilis (Onagraceae).New Phytologist.https://doi.org/10.1111/nph.12062

Wang Z, Li X, Chen M, et al (2023) Molecular and Metabolic Insights into Anthocyanin Biosynthesis for Spot Formation on Lilium leichtlinii var. maximowiczii Flower Petals. Int J Mol Sci.https://doi.org/10.3390/ijms24031844

Li X , Li Y , Zhao M ,et al (2023) Molecular and Metabolic Insights into Anthocyanin Biosynthesis for Leaf Color Change in Chokecherry (Padus virginiana).International journal of molecular sciences.https://doi.org/10.3390/ijms221910697

Ma D, Constabel C P (2019) MYB Repressors as Regulators of Phenylpropanoid Metabolism in Plants.Trends in Plant Science.https://doi.org/10.1016/j.tplants.2018.12.003

An JP, Qu FJ, Yao JF, et al (2017) The bZIP transcription factor MdHY5 regulates anthocyanin accumulation and nitrate assimilation in apple. Hortic Res. https://doi.org/10.1038/hortres

Cong L, Qu Y, Sha G, et al (2021) PbWRKY75 promotes anthocyanin synthesis by activating PbDFR, PbUFGT, and PbMYB10b in pear. Physiol Plant.https://doi.org/10.1111/ppl.13525

Zhang S, Chen Y, Zhao L, et al (2020) A novel NAC transcription factor, MdNAC42, regulates anthocyanin accumulation in red-fleshed apple by interacting with MdMYB10. Tree Physiol. https://doi.org/10.1093/treephys/tpaa004

Liu H, Liu Z, Wu Y, et al (2021) Regulatory Mechanisms of Anthocyanin Biosynthesis in Apple and Pear. Int J Mol Sci.https://doi.org/10.3390/ijms22168441

Lichtenthaler HK, Wellburn AR (1983) Determinations of total carotenoids and chlorophylls a and b of leaf extracts in different solvents.Analysis.https://doi.org/10.1042/bst0110591

Dubos C, Stracke R, Grotewold E,et al (2010) MYB transcription factors in Arabidopsis [Review].Trends in Plant Science.https://doi.org/10.1016/j.tplants.2010.06.005

Zhang X, Zhang L, Zhang D, et al (2023) Comprehensive analysis of metabolome and transcriptome reveals the mechanism of color formation in different leave of Loropetalum Chinensevar.Rubrum.BMC Plant Biology.https://doi.org/10.1186/s12870-023-04143-9

Jiang G, Li Z, Song Y, et al (2019) LcNAC13Physically Interacts with LcR1MYB1 to Coregulate Anthocyanin Biosynthesis-Related Genes during Litchi Fruit Ripening. Biomolecules. https://doi.org/10.3390/biom9040135

Zhang B, Zhang M, Jia X, et al (2023) Integrated Transcriptome and Metabolome Dissecting Interaction between Vitis vinifera L. and Grapevine Fabavirus. Int J Mol Sci. https://doi.org/10.3390/ijms24043247

Lu L, Yang W, Dong Z, et al (2023) Integrated Transcriptomic and Metabolomics Analyse Reveal Molecular Responses to Cold Stress in Coconut(Cocos nucifera L.) Seedlings. Int J Mol Sci. https://doi.org/ 10.3390/ijms241914563

Wen L, Liu T, Deng Z, et al (2022) Characterization of NAC transcription factor NtNAC-028 as a regulator of leaf senescence and stress responses. Front Plant Sci. https://doi.org/10.3389/fpls.2022.941026

Ooka, H (2003) Comprehensive analysis of NAC family genes in Oryza sativa and Arabidopsis thaliana.DNA research.https://doi.org/10.1093/dnares/10.6.239

Li T, Fan Y, Qin H, et al (2020) Transcriptome and Flavonoids Metabolomic Analysis Identifies Regulatory Networks and Hub Genes in Black and White Fruits of Lycium ruthenicum Murray.Frontiers in Plant Science.https://doi.org/10.3389/fpls.2020.01256

Morishita T, Kojima Y, Maruta T, et al (2014) Arabidopsis NAC transcription factor, ANAC078 regulates flavonoid biosynthesis under high-light.Nano Letters.https://doi.org/10.1021/nl503125u

Sun Q, Jiang S, Zhang T, et al (2019) Apple NAC transcription factor MdNAC52 regulates biosynthesis of anthocyanin and proanthocyanidin through MdMYB9 and MdMYB-11. Plant Science.https://doi.org/10.1016/j.plantsci.2019.110286

Xu W, Grain D, José LG, et al (2013) Regulation of flavonoid biosynthesis involves an

unexpected complex transcriptional regulation of TT8 expression, in Arabidopsis. New Phytologist.https://doi.org/10.1111/nph.12142

Zhou X, Xue Y, Mao M, et al (2021) Metabolome and transcriptome profiling reveals anthocyanin contents and anthocyanin-related genes of chimeric leaves in Ananas comosus var. bracteatus.BMC Genomics.https://doi.org/10.1186/S12864-021-07642-X

Zou J, Gong Z, Liu Z, et al (2023) Investigation of the Key Genes Associated with Anthocyanin Accumulation during Inner Leaf Reddening in Ornamental Kale (Brassica oleracea L. var. acephala. Int J Mol Sci. https://doi.org/ 10.3390/ijms24032837

Wei H, Chen X, Zong X, et al (2015) Comparative Transcriptome Analysis of Genes Involved in Anthocyanin Biosynthesis in the Red and Yellow Fruits of Sweet Cherry (Prunus avium L.).Plos One.https://doi.org/10.1371/journal.pone.0121164

Yao X, Yao Y, An L, et al (2022) Accumulation and regulation of anthocyanins in white and purple Tibetan Hulless Barley (Hordeum vulgare L. var. nudum Hook. f.) revealed by combined de novo transcriptomics and metabolomics. BMC Plant Biol. https://doi.org/ 10.1186/s12870-022-03699-2

Li Y, Kong F, Liu Z, et al (2022) PhUGT78A22, a novel glycosyltransferasein Paeonia 'He Xie', can catalyze the transfer of glucose to glucosylated anthocyanins during pe-tal blotch formation. BMC Plant Biol. https://doi.org/ 10.1186/s12870-022-03777-5

Xue X, Duan Y, Wang J, et al (2021) Nighttime Temperatures and SunlightIntensities Interact to Influence Anthocyanin Biosynthesis and PhotooxidativeSunburn in 'Fuji' Apple. Front Plant Sci.https://doi.org/10.3389/fpls.2021.694954

Wen XC, Han J, Leng XP, et al (2014) Cloning and expression of UDP-glucose: flavonoid3-O-glucosyltransferase gene in peach flowers. Genet MolRes. https://doi.org/ 10.4238/2014.December.4.1

Koyama R, Roberto SR, de SRT, et al (2018) Exogenous Abscisic Acid Promotes Anthocyanin Biosynthesis and Increased Expression of Flavonoid Synthesis Genes In Vitis vinifera × Vitis labrusca Table Grapes in a Subtropical Region. Front Plant Sci. https://doi.org/ 10.3389/fpls.2018.00323

Ni X, Xue S, Iqbal S, et al (2018) Candidate genes associated with red colour formation revealed by comparative genomic variant analysis of red- and green-skinned fruits of Japanese apricot (Prunus mume). PeerJ. https://doi.org/ 10.7717/peerj.4625

Zhao ZC, Hu GB, Hu FC, et al (2012) The UDP glucose:flavonoid-3-O-glucosyltransferase (UFGT) gene regulates anthocyanin biosynthesisin litchi (Litchi chinesis Sonn.) during fruit coloration. Mol Biol Rep. https://doi.org/ 10.1007/s11033-011-1303-3

Morita Y, Takagi K, Fukuchi-Mizutani M, et al (2014) A chalcone isomerase-like protein enhances flavonoid production and flower pigmentation. Plant Journal.https://doi.org/10.1111/tpj.12469

Ryan KG, Swinny EE, Markham KR, et al (2002) Flavonoid gene expression and UV photoprotection in transgenic and mutant Petunia leaves.Phytochemistry.https://doi.org/10.1016/s0031-9422(01)00404-6

Xing WZ , Ji YL , Yu LZ ,et al (2017) De novo Assembly of the Camellia nitidissima Transcriptome Reveals Key Genes of Flower Pigment Biosynthesis. Frontiers in Plant Science.https://doi.org/10.3389/fpls.2017.01545

Hong ZZ, Lin Z, Lu LH, et al (2022) transcriptome profi1ing revea1s the ro1es of pigment fonnation mechanisms in ye11ow paeonia de1avayi f1owers. Molecular Genetics and Genomics.https://doi.org/10.1007/s00438-022-01973-4

Gonzalez A, Zhao M, Leavitt JM, et al (2010) Regulation of the anthocyanin biosynthetic pathway by the TTG1/bHLH/Myb transcriptional complex in Arabidopsis seedlings. Plant Journal.https://doi.org/10.1111/j.1365-313X.2007.03373.x

Stracke R, Ishihara H, Huep G, et al (2010) Differential regulation of closely related R2R3-MYB transcription factors controls flavonol accumulation in different parts of the Arabidopsis thaliana seedling.Plant Journal.https://doi.org/10.1111/j.1365-313X.2007.03078.x

Espley RV, Brendolise C, Chagne D, et al (2009) Multiple Repeats of a Promoter Segment Causes Transcription Factor Autoregulation in Red Apples.Plant Cell.https://doi.org/10.1105/tpc.108.059329

Wen CH, Chu FH (2017) A R2R3-MYB Gene LfMYB113 is Responsible for Autumn Leaf Coloration in Formosan sweet gum (Liquidambar formosana Hance). PLANT CELL PHYSIOL.https://doi.org/10.1093/pcp/pcw228

Zou SC, Zhuo MG, Abbas F, et al (2023) Transcription factorLcNAC002 coregulates chlorophyll degradation and anthocyanin biosynthesis in litchi. Plant Physiol. https://doi.org/10.1093/plphys/kiad118

Zhou H, Kui LW, Wang H, et al (2015) Molecular genetics of blood-fleshed peach reveals activation of anthocyanin biosynthesis by NAC transcription factors.The Plant Journal. https://doi.org/10.1111/tpj.12792

D'Incà E, Foresti C, Orduña L, et al (2023) The transcription factor VviNAC60 regulates senescence and ripening-related processes in grapevine. Plant Physiol. https://doi.org/10.1093/plphys/kiad050

Xu T, Yu L, Huang N, et al (2023) The regulatory role of MdNAC14-Like in anthocyani nsynthesis and proanthocyanidin accumulation in red-fleshed apples. Plant PhysiolBiochem. https://doi.org/ 10.1016/j.plaphy.2023.108068

Zhong R, Lee C, Zhou J, et al (2008) A battery of transcription factors involved in the regulation of secondary cell wall biosynthesis in Arabidopsis. Plant Cell. https://doi.org/10.1105/tpc.108.061325

Yan H, Pei X, Zhang H, et al (2021) MYB-Mediated Regulation of Anthocyanin Biosynthesis.International Journal of Molecular Sciences.https://doi.org/10.3390/ijms22063103

Tian Y, Rao S, Li Q, et al (2021) The coloring mechanism of a novel golden variety in Populus deltoides based on the RGB color mode.Forestry Research.https://doi.org/10.48130/FR-2021-0005

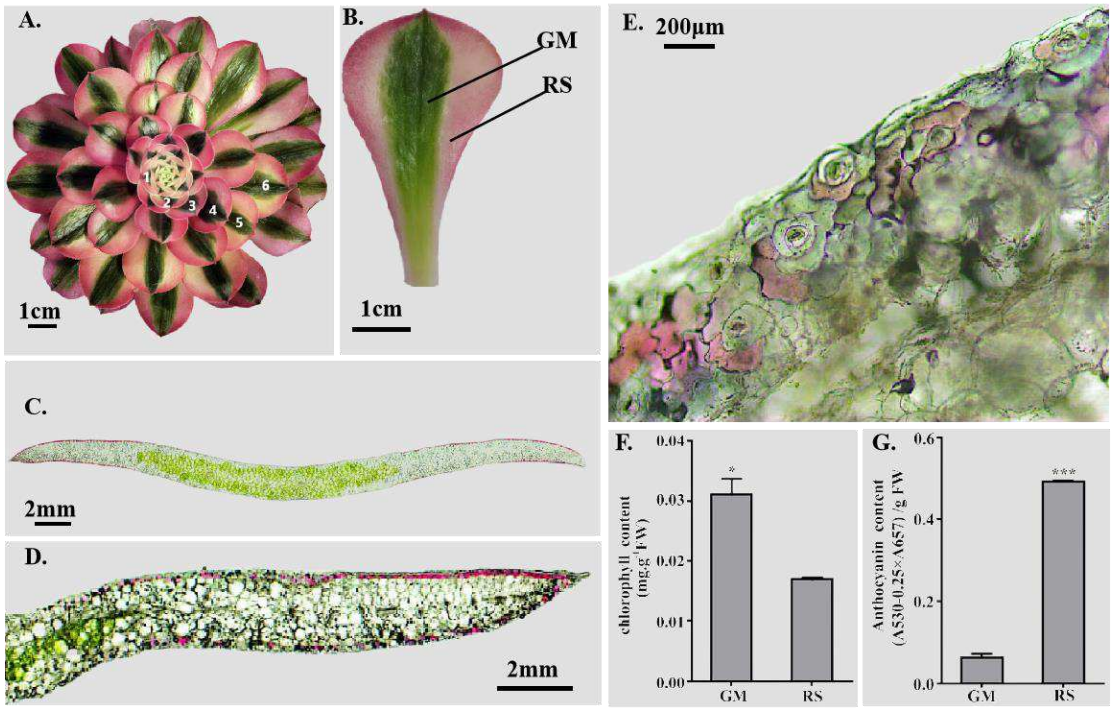

Fig. 1 The physiological parameters and leaf color distribution of *Aeonium arboreum* 'Pink Sybil'. **A** Full plant morphology. **B** Sampling sites include GM and RS. **C** The distribution of anthocyanins and chlorophyll in a whole leaf cross-section was observed using a 4×/0.10 NA objective. **D** Using a 10×/0.22NA objective, a cross-section of the central and marginal regions of the leaf demonstrates that anthocyanins are largely located in the cells of 1-2 layers below the epidermis in the RS region. **E** Guard cells and pigment cells were seen in the anthocyanin concentration area with 40×/0.65NA objective microscopy. **F** The total quantity of chlorophyll. G. Content of anthocyanins. The student t-test revealed statistically significant differences (* $P < 0.05$, *** $P < 0.001$). The results are shown as the averages of three replicates, with error bars indicating the standard deviation (±).

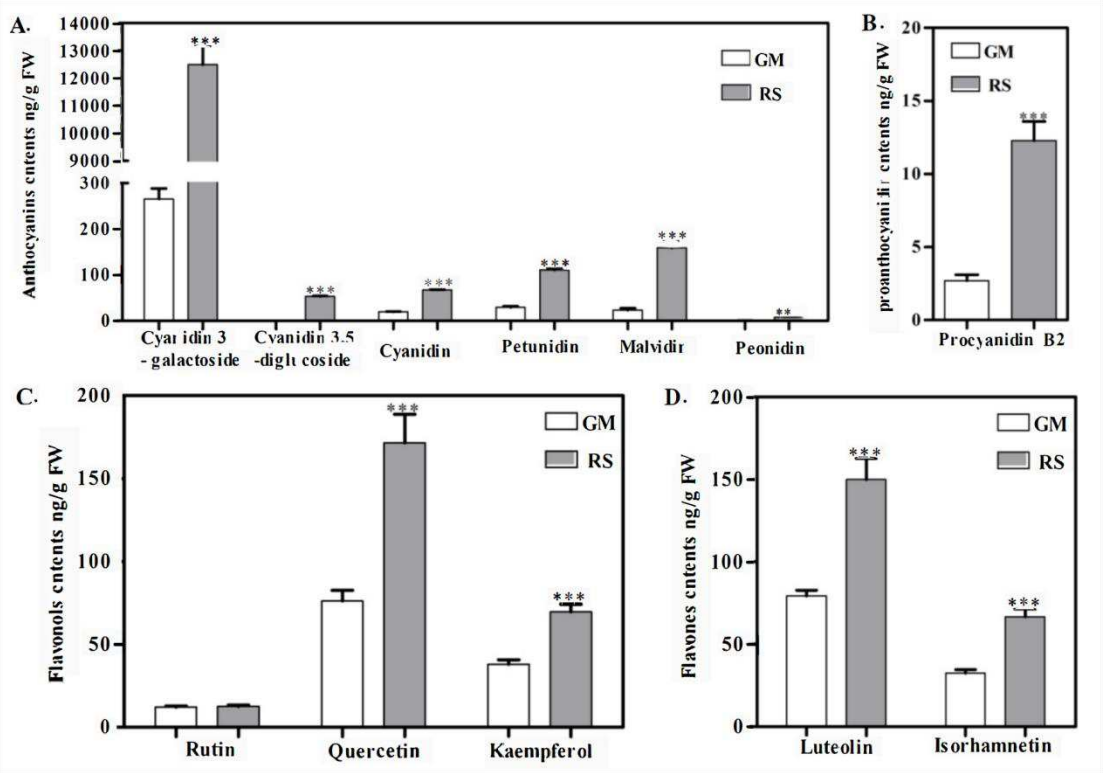

Fig. 2 Qualitative and quantitative analysis of flavonoids in 'Pink Sybil' leaves. **A** Anthocyanins content. **B** procyanidin B2 content. **C** Flavonols content. **D** Flavonoids content. The student's t-test (*** $P < 0.001$) revealed significant differences. The results are shown as the averages of three replicates, with error bars indicating the standard deviation (±).

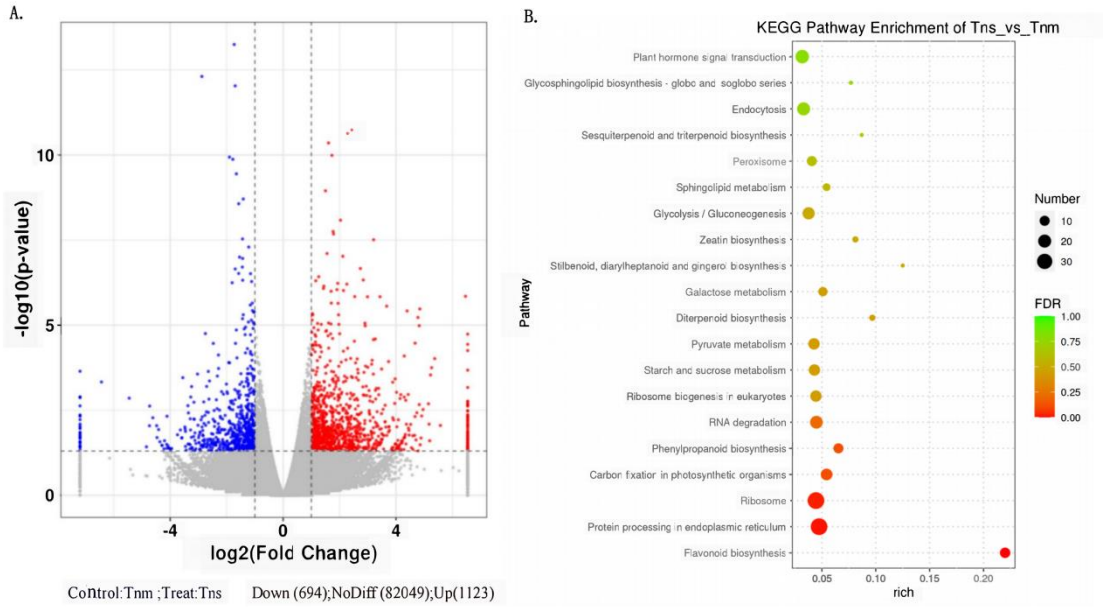

Fig. 3 Volcano plot and KEGG pathway between Tnm (GM) and Tns (RS). **A** Volcano plot of 'Pink Sybil' leaf Tnm (GM) and Tns (RS). The DEG criteria: |log2FoldChange| > 1. Blue dots indicate down-regulated genes, whereas red dots indicate up-regulated genes. **B** The vertical and horizontal axes depict DEG enrichment along the KEGG pathway between Tnm (GM) and Tns (RS) in the leaves of the 'Pink Sybil'.

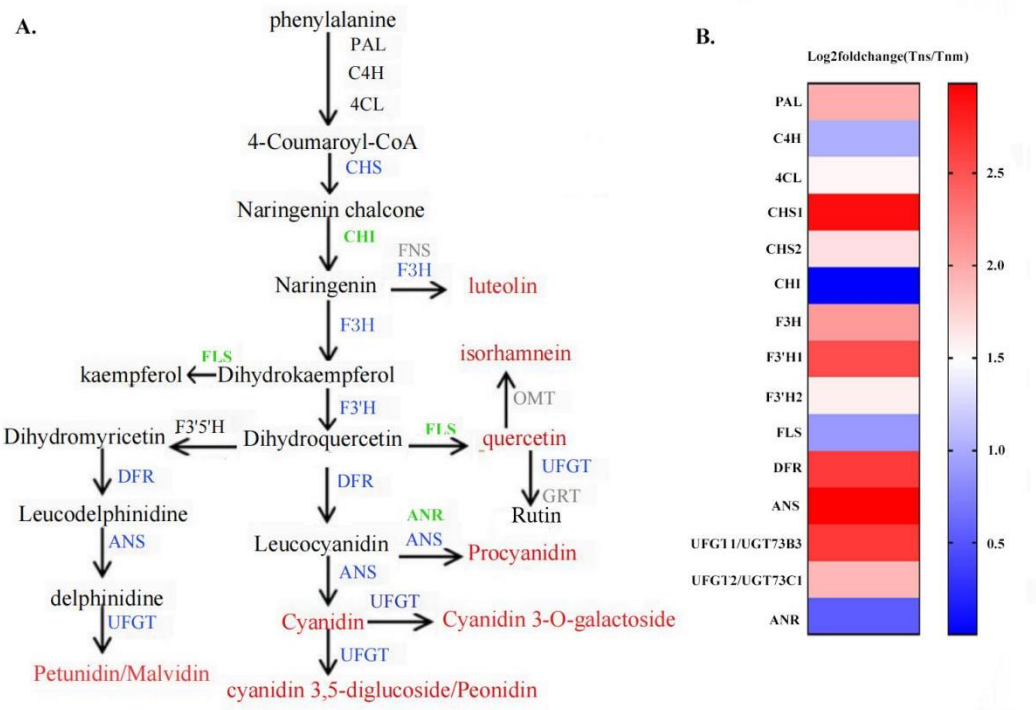

Fig. 4 Heat map of structural genes associated with flavonoid production and schematic diagram of the 'Pink Sybil' flavonoid synthesis pathway. In Fig. 4A, red font indicates up-regulated differently expressed metabolites, blue font indicates up-regulated differentially expressed structural genes, green font indicates up-regulated but not statistically different structural genes, and gray font indicates no up-regulation of structural genes. The log-transformed RPKM values are shown on the color scale in Fig. 4B.

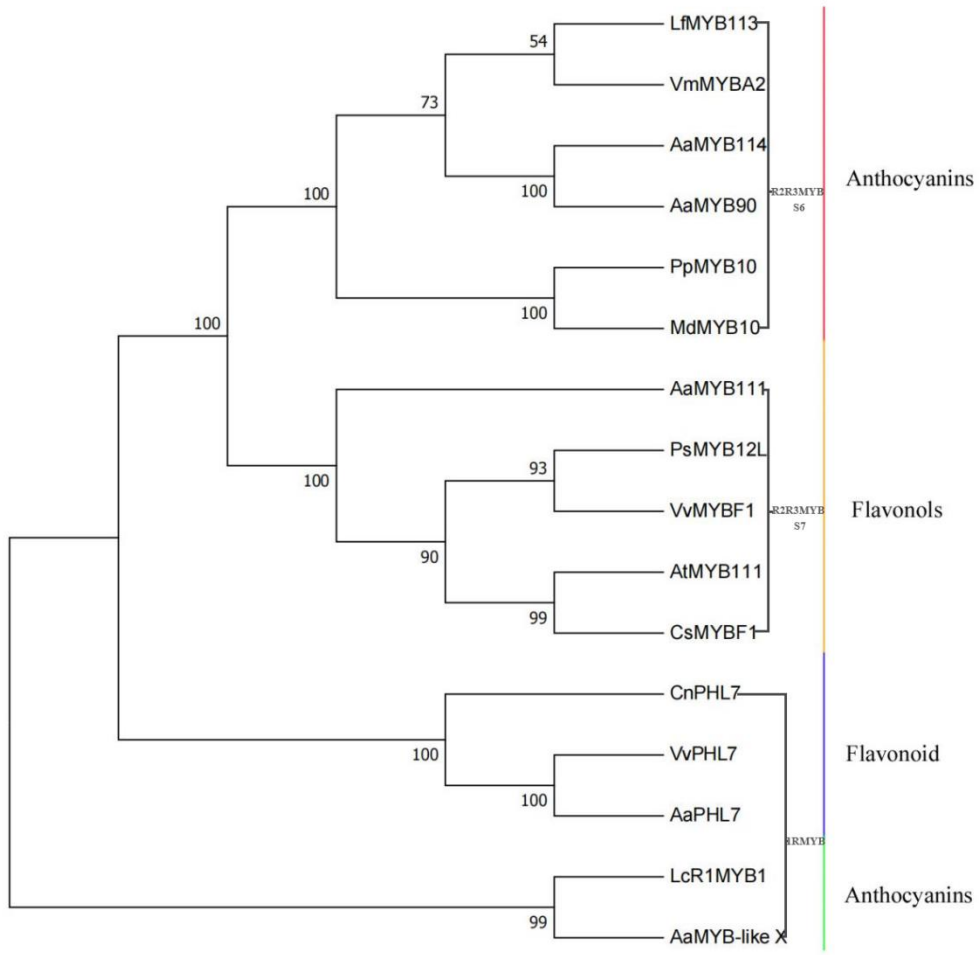

Fig. 5 Phylogenetic analysis of MYB transcription factors in 'Pink Sybil' and other species that synthesize flavonoids. Using MEGA 7, p-distance models were built using the neighbor-joining approach (self-help test with 1000 replications). Lf, *Liquidambar formosana* Hance; Vm, Vaccinium; Aa, *Aeonium arboretum* 'Pink Sybil'; Pp, *Prunus persica*; Md, *Malus domestica*; Ps, *Paeonia suffruticosa*; Vv, *Vitis vinifera*; At, *Arabidopsis thaliana*; Cs, *Citrus sinensis*; Cn, *Cocos nucifera*; Lc, *Litchi chinensis*.

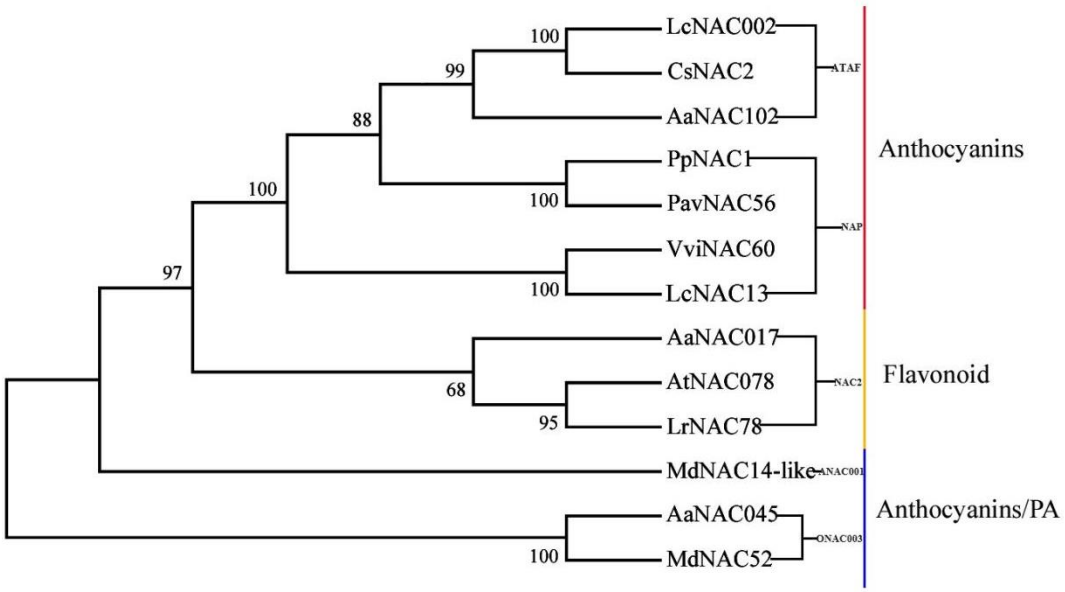

Fig. 6 Phylogenetic analysis of NAC transcription factors in 'Pink Sybil' and other species that synthesize flavonoids. Using MEGA 7, p-distance models were built using the neighbor-joining approach (self-help test with 1000 replications). Lc, *Litchi chinensis*; Cs, *Citrus sinensis*; Aa, *Aeonium arboretum* 'Pink Sybil'; Pp, *Prunus persica*; Pav, *Prunus avium*; Vv, *Vitis vinifera*; At, *Arabidopsis thaliana*; Lr, *Lycium ruthenicum*; Md, *Malus domestica*.

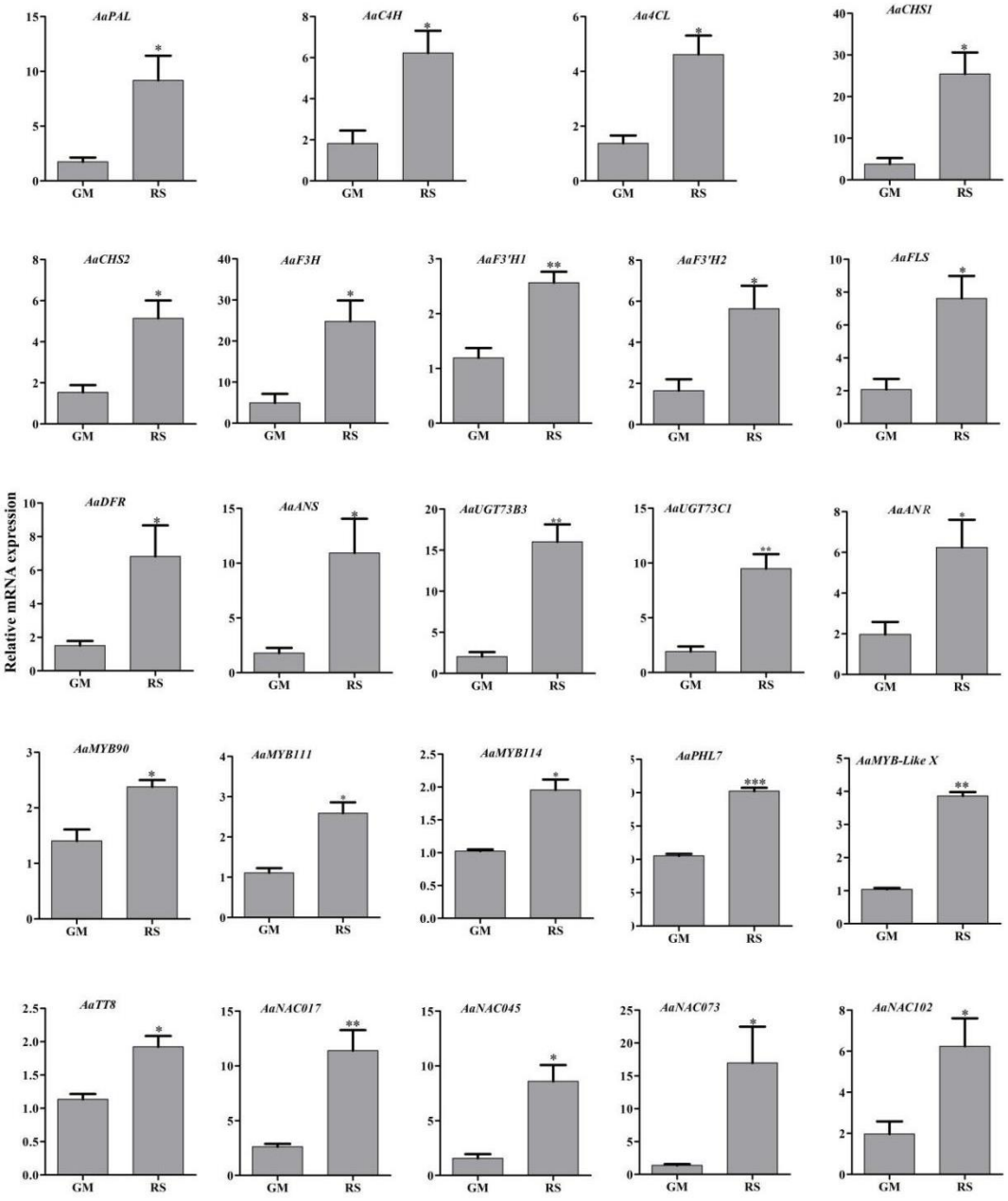

Fig. 7 'Pink Sybil'leaf flavonoid synthesis: qPCR validation of transcription factors and differentially expressed structural genes. * above the RS bars indicates $0.01 \leq P < 0.05$; ** suggests $0.001 \leq P < 0.01$; and *** shows $P < 0.001$, as determined by the student's t-test. Data are shown as the mean of three replicates, with error bars indicating ± SD.

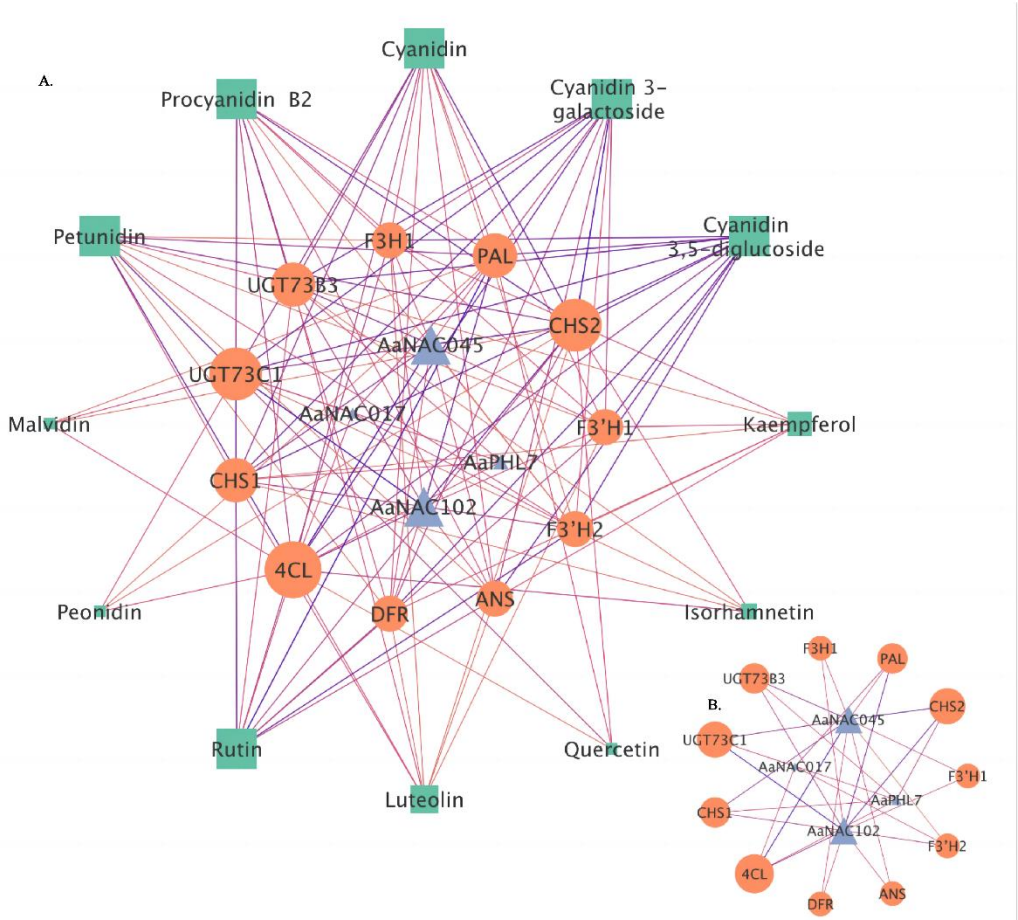

C.

0.9411	0.9411	0.9411	0.9411	0.9411	0.9411	0.8804	0.9411	0.9411	0.9411	0.9411	Cyanidin 3,5-diglucoside
1.0000	0.8286	0.8286	0.9429	0.9429	0.9429	0.9429	0.8286	0.8286	0.7714	0.8286	Cyanidin 3- galactoside
0.9429	0.7714	0.7714	0.8857	0.8857	0.8857	0.8286	0.7714	0.7714	0.7143	0.7714	Cyanidin
0.9429	0.7714	0.7714	0.8857	0.8857	0.8857	0.8286	0.7714	0.7714	0.7143	0.7714	Procyanidin B2
0.8857	0.8857	0.7143	0.7714	0.9429	0.7714	0.9429	0.7143	0.7143	0.7714	0.7143	Petunidin
0.7143	0.7143			0.7714		0.7714					Malvidin
0.7143	0.7143			0.7714		0.7714					Peonidin
0.8286	1.0000	0.8286	0.7714	0.9429	0.7714	0.7714	0.8286	0.8286	0.9429	0.8286	Rutin
0.7143		0.7143	0.7714		0.7714	0.7714	0.7143	0.7143		0.7143	Luteolin
0.7714	0.7714			0.8286		0.7143					Quercetin
0.7714			0.7143	0.7143	0.7143	0.8286					Isorhamnetin
		0.7714	0.7143		0.7143		0.7714	0.7714	0.7143	0.7714	Kaempferol
0.9429	0.7714	0.7714	0.8857	0.8857	0.8857	1.0000	0.7714	0.7714	0.7143	0.7714	AaNAC045
	0.8286			0.7714		0.7714			0.7714		AaNAC017
0.9429	0.9429	0.7714	0.8286	1.0000	0.8286	0.8857	0.7714	0.7714	0.8286	0.7714	AaNAC102
0.8286			0.7714	0.7714	0.7714	0.7714					AaPHL7
CHS2	PAL	F3H1	UGT73B3	UGT73C1	CHS1	4CL	DFR	ANS	F3'H2	F3'H1	

D.

Fig. 8 Metabolites linked to anthocyanin synthesis and transcriptome association research. **A** Plots depict the network relationships between structural genes, transcription factors, and key metabolites. **B** Key transcription factors and structural genes are displayed beside one another.

C Correlation coefficients for transcription factors, structural genes, and metabolites involved in anthocyanin synthesis. **D** color reference for the line between nodes based on the correlation.

Supplementary Files

This is a list of supplementary files associated with this preprint. Click to download.

- SUPPLEMENTARYINFORMATION.pdf